Continental Shelf Research 28 (2008) 1424–1434

Contents lists available at ScienceDirect

Continental Shelf Research

journal homepage: www.elsevier.com/locate/csr

Seasonal variations in the inorganic carbon system in the Pearl River (Zhujiang) estuary

Xianghui Guo [a,b], Wei-Jun Cai [b,*], Weidong Zhai [a], Minhan Dai [a], Yongchen Wang [b], Baoshan Chen [a]

[a] State Key Laboratory of Marine Environmental Science, Xiamen University, Xiamen 361005, China
[b] Department of Marine Sciences, University of Georgia, GA 30602, USA

ARTICLE INFO

Article history:
Received 22 April 2006
Received in revised form
24 April 2007
Accepted 21 July 2007
Available online 13 March 2008

Keywords:
Pearl River estuary
Estuarine mixing
Dissolved inorganic carbon

ABSTRACT

Seasonal variations in the inorganic carbon system in the Pearl River estuary are examined based on data from five surveys during the spring, summer, fall, and winter seasons. Both total dissolved inorganic carbon (DIC) and total alkalinity (TAlk) values in the freshwater end-members are high in the dry season ($>2700\,\mu mol\,kg^{-1}$ for DIC and $>2400\,\mu mol\,kg^{-1}$ for TAlk) and substantially lower in the wet season (DIC and TAlk were ~1000 and 700 $\mu mol\,kg^{-1}$, respectively). Riverine DIC flux and drainage basin weathering rates, however, are significantly higher in the wet season ($611\times10^9\,mol\,yr^{-1}$ and $13.6\times10^5\,mol\,km^{-2}\,yr^{-1}$) than in the dry season ($237\times10^9\,mol\,yr^{-1}$ and $5.3\times10^5\,mol\,km^{-2}\,yr^{-1}$).

In the estuarine mixing zone, DIC and TAlk are generally conservative at salinities >5, while in the low-salinity zone the carbonate system shows a much more complex distribution pattern. In the dry season, DIC and TAlk show a decreasing pattern with salinity, while they have an increasing pattern in the wet season. This complex behavior is mainly a result of mixing between tributaries with distinct and seasonally variable DIC and TAlk values. Distributions of inorganic carbon parameters, in particular pH and pCO_2, are however noticeably modified by local acid-generating biogeochemical processes in the upper estuary. Processes such as nitrification increase acidity during the dry season when freshwater discharge is low and NH_4^+-rich pollutant discharge from the neighboring metropolitan areas is relatively high.

1. Introduction

About 1×10^{15} g of carbon is discharged annually from the land to the ocean through rivers and estuaries (Degens et al., 1991), of which 40% is dissolved inorganic carbon (DIC) (Richey et al., 2002 and references therein). Atmospheric CO_2 is sequestered into terrestrial systems through photosynthesis and weathering reactions and, together with mineral materials, is transported to the ocean via rivers. A knowledge of DIC fluxes from various drainage basins via rivers, particularly from large rivers and their modulation are important for a better understanding of global biogeochemical cycling.

In principle, the supply of inorganic carbon by a river is controlled by weathering intensity and local geology at its drainage basin. DIC concentrations and/or total alkalinity (TAlk) values and their fluxes in the estuarine zone are subject to considerable seasonal variation due to changes in precipitation and weathering rates in the drainage basins and upper streams (Cai, 2003; Probst et al., 1992). The fluxes of DIC and TAlk may also be subject to modification within estuaries characterized by strong physicochemical gradients, enhanced biological activity, and intense sedimentation and/or re-suspension (Abril and Borges, 2004; Frankignoulle et al., 1998), which add to the complexity of seasonal DIC/TAlk fluxes from rivers to the oceans.

However, studies on the seasonal variation of inorganic carbon systems in the estuarine zones of the world's major rivers are still very limited. This is especially true for Asian rivers, despite the fact that both freshwater discharge and DIC export from Asia may be the highest among all the continents (Degens et al., 1991). The Pearl River and the Mekong are the two largest rivers discharging into the South China Sea (SCS), the largest marginal sea of the northwestern Pacific Ocean.

In this paper, the seasonal variation of the inorganic carbon system in the Pearl River estuary is investigated based on data collected from five cruises covering all seasons of the year. Control mechanisms of the carbonate system which drive the seasonal variation are examined in detail.

2. Materials and methods

2.1. Study area

The Pearl River drainage basin is located in a sub-tropical climate zone in Southwestern China (Fig. 1). It has an annual freshwater discharge of $3.26\times10^{11}\,m^3$, and ~80% of the discharge

* Corresponding author. Tel.: +1 706 254 8438.
E-mail address: wcai@uga.edu (W.-J. Cai).

0278-4343/$ - see front matter © 2008 Elsevier Ltd. All rights reserved.
doi:10.1016/j.csr.2007.07.011

takes place in the wet season driven by the Asian monsoon (April–October) (Fig. 2). The river has three major tributaries, namely the Xijiang (also known as Si Kiang in literature, meaning West River), Beijiang (North River) and Dongjiang (East River), as well as several small local rivers (Fig. 1). Amongst them, the West River accounts for ~70% of the total freshwater discharge. All runoffs from these tributaries discharge into the SCS via eight major outlets: Humen, Jiaomen, Hongqimen, Hengmen, Modaomen, Jitimen, Hutiaomen and Yamen (Zhao, 1990) and through three sub-estuaries: Lingdingyang, Modaomen and Huangmaohai. This study focuses on the Humen Outlet and the Lingdingyang, which is traditionally regarded as the Pearl River estuary. The Lingdingyang is fed by the East River, the North River and part of the West River, as well as some small rivers in the deltaic area (Zhao, 1990; PRWRC/PRRCC, 1991) (Fig. 1).

The Pearl River has been subjected to intense anthropogenic disturbance for a long time and it receives an annual wastewater discharge of $\sim 5000 \times 10^6$ tons yr^{-1} from upstream cities such as Guangzhou, Foshan and Dongguan in recent years (see the Environmental Status Bulletins of Guangdong Province, China; http://www.gdepb.gov.cn/). Associated with these high waste discharges, high partial pressures of CO_2 (pCO_2) and low dissolved oxygen (DO) have been observed in the upper Pearl River estuary (Zhai et al., 2005; Dai et al., 2006), which have a clear impact on the inorganic carbon system.

2.2. Sampling

DIC, TAlk, pH and auxiliary data (salinity, temperature, wind speed, barometric pressure, etc.) were collected in July 2000, May–June 2001, November 2002, and February 2004, representing summer, spring, fall and winter, respectively. Water column samples were collected with a SEACAT CTD rosette system equipped with 1.7-L Niskin/2.6-L Go-Flo bottles on board R.V. *Yanping II*. Discrete underway sampling was conducted via a side vent of the pCO_2-DO pumping system (see details in Zhai et al., 2005; Dai et al., 2006). Samples were also collected in January 2005 with 2.6-L Go-Flo bottles for water columns and from a side vent of the pCO_2-DO underway pumping system for some surface water samples on a small boat. These samples covered a salinity gradient from 0 to >30 (sampling sites for water column samples are dotted on the map; Fig. 1B). Samples for the inorganic carbon system (DIC, TAlk and pH) were free of air bubbles and stored in glass bottles until analysis.

2.3. Analysis

Temperature and salinity (conductivity) were measured using two SEACAT thermosalinograph systems (CTD; SBE21 for underway samples and SBE19 for water column samples, Sea-Bird Co.) for the first four cruises, and with a Yellow Spring Instrument meter (YSI 6600) in January 2005. Salinity was also verified against chlorinity determined by $AgNO_3$ titration (Millero, 1984; Grasshoff et al., 1999).

DIC and TAlk were determined within a week of sampling (after preservation with saturated $HgCl_2$ in July 2000 and May–June 2001) or within 24 h of sampling (DIC in November 2002, February 2004 and January 2005). The analytical methods of DIC and TAlk have been described in Cai et al. (2004) and each has a precision of $\pm 2\,\mu mol\,kg^{-1}$. Certified reference materials from A.G. Dickson of Scripps Institution of Oceanography (CRM Batch 46# for July 2000, May 2001 and November 2002, Batch 60# for February 2004 and Batch 65# for January 2005) were used for calibration. Unfortunately, during the November 2002 survey, the DIC analyzer failed after a limited number of measurements.

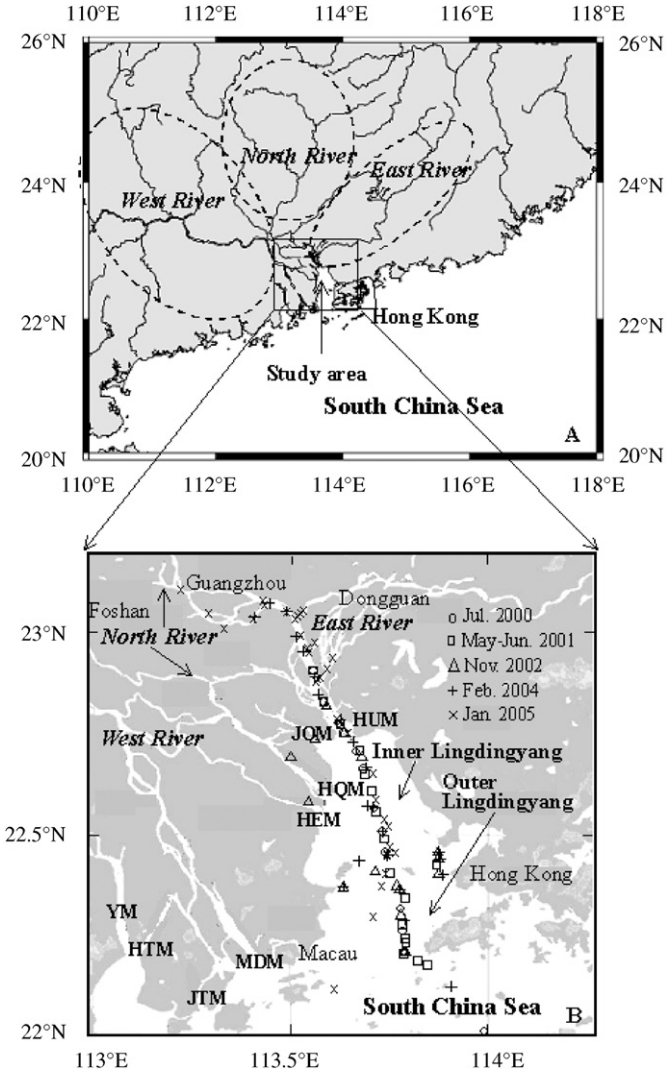

Fig. 1. Maps of the Pearl River estuary and survey stations. The areas circled are the West River, North River and East River on panel (A). HUM, JOM, HQM, HEM, MDM, JTM, HTM and YM denote Humen, Jiaomen, Hongqimen, Hengmen, Modaomen, Jitimen, Hutiaomen and Yamen, respectively, on panel (B).

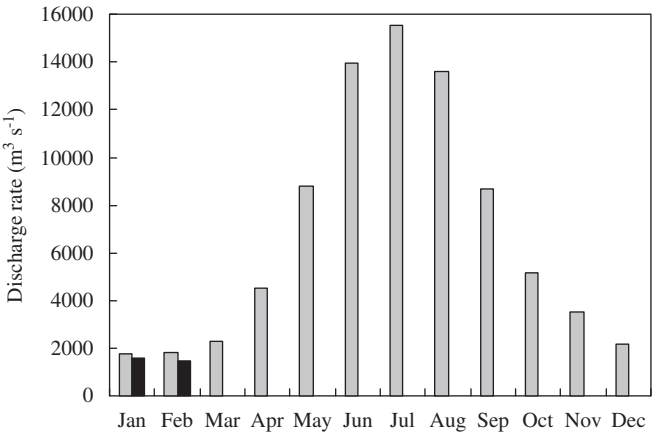

Fig. 2. Water discharge rate at the Wuzhou hydrological station on the West River (http://sqqx.hydroinfo.gov.cn/websq/). Gray bars are the long-term monthly averaged discharge and the black bars are the average discharge of January 2005 and February 2004, which are ~11% and ~20% lower than the long-term average, respectively.

Table 1
Effective DIC and TAlk values and their fluxes in the Pearl River estuary

Survey period	DIC (TAlk) (μmol kg^{-1}) as a function of salinity	Effective values (μmol kg^{-1})	Monthly averaged discharge ($m^3 s^{-1}$)[a]	DIC flux (10^9 mol yr^{-1})	TAlk flux (10^9 mol yr^{-1})
July 2000	DIC = 12.08 × S+1523, R^2 = 0.79, n = 38	1523	22,203	1066.4	1110.5
	TAlk = 18.83 × S+1586, R^2 = 0.91, n = 26	1586			
May–June 2001	DIC = 13.78 × S+1321, R^2 = 0.84, n = 31	1321	12,457	519.0	467.5
	TAlk = 31.90 × S+1190, R^2 = 0.79, n = 28	1190			
November 2002	DIC = 12.61 × S+1550, R^2 = 0.94, n = 16	1550	5024	245.6	212.6
	TAlk = 27.77 × S+1342, R^2 = 0.96, n = 42	1342			
February 2004	DIC = 5.945 × S+1840.0, R^2 = 0.73, n = 22	1840	2114	122.7	109.5
	TAlk = 19.24 × S+1643, R^2 = 0.97, n = 20	1643			
January 2005	DIC = −10.990 × S+2306.7, R^2 = 0.73, n = 35	2307	2571	187.1	171.4
	TAlk = 2.62 × S+2114, R^2 = 0.48, n = 22	2114			

[a] Hydrological Department of China, http://sqqx.hydroinfo.gov.cn/websq.

Therefore, only those few DIC measurements made within 24 h of collection were used for the calculation of the effective freshwater DIC value for this cruise (Table 1). Considering the fact that these limited DIC data have a good linear correlation with TAlk (n = 12, R^2 = 0.89), we estimated other DIC values from the relationship between DIC and TAlk, but only present them in Fig. 3B and Fig. 4A for qualitative discussion.

pH was measured immediately after sample collection using a Corning® pH/ion analyzer 350 and a Ross combination electrode (Orion®), which was calibrated against three NIST-traceable pH buffers (pH 4.01, 7.00 and 10.01 at 25 °C) just prior to and after every series of measurements. Precision of pH measurements was ±0.005. The in situ pH values were calculated based on Gieskes (1969) empirical temperature effect coefficient via Eq. (1):

$$pH_{in\ situ} = pH_{meas.} + 0.0114(T_{meas.} - T_{in\ situ}), \quad (1)$$

where $pH_{in\ situ}$ and $pH_{meas.}$ are the pH values at the in situ temperature ($T_{in\ situ}$) and at the measurement temperature ($T_{meas.}$), respectively.

3. Results

3.1. Hydrological settings

The salinity in the vicinity of the Humen Outlet (distance = 0 in Fig. 3) was 0–3 in July 2000, May–June 2001 and November 2002, but was >15 in February 2004 and January 2005 (Fig. 3A), reflecting the greatly different discharge rates between the wet and dry seasons. The freshwater end-member was located 0–20 km upstream of Humen in July 2000 and May–June 2001, but it moved to ~50 km upstream of Humen in February 2004 and was near Guangzhou. The spatial distribution of salinity in the Lingdingyang was highly variable due to the freshwater discharge from several main outlets. The surface temperature of the surveyed area in July 2000, May–June 2001, November 2002, February 2004 and January 2005 was 27.6–31.2, 25.9–28.5, 21.1–24.3, 14.3–17.4 and 14.5–16.9 °C, respectively. For the convenience of discussion hereafter, and based on the spatial distribution of salinity and the flow rate of the river, July 2000 and May–June 2001 are regarded as wet season cruises, November 2002 as a transitional season, and February 2004 and January 2005 as dry season cruises.

A 3-day plume travel time was reported for the Lingdingyang (Wong and Cheung, 2000), but no water transit time for the inner estuary upper stream of the Humen was reported. Based on the width of the river channel (http://www.gzsdfz.org.cn), we calculated an annual mean total volume of water between our uppermost station just north of Guangzhou and Humen as 7.5×10^8 m^3. As the daily mean discharge rate through Humen is 1.5×10^8 m^3 d^{-1} (Cai et al., 2004), we estimated a yearly mean water transit time of 5 days. It was not known how these parameters vary between dry and wet seasons. For the purpose of comparison and discussion in this paper, we assumed a water transit time of 5–10 days for the section between northern Guangzhou and Humen in the dry season.

3.2. Spatial distributions of DIC and TAlk

The end-member values and the distributions of DIC, TAlk, and pH in the estuarine zone show a significant seasonal variability (Fig. 3B, C and D). DIC in the freshwater end-member was low in spring and summer (wet season) (798–1572 μmol kg^{-1} at 20 km upstream of Humen) and increased downstream. In contrast, the upper estuary had very high DIC levels in the freshwater end-member in February 2004 and January 2005 (winter and dry season) (2744–3329 μmol kg^{-1} at ~50–70 km upstream of Humen) and decreased rapidly downstream in the upper estuarine zone (30–70 km upstream of Humen). A DIC minimum ~30 km upstream of Humen was observed in February 2004, but not in January 2005. The distribution patterns of TAlk were similar to those of DIC, with values of 746–1570 μmol kg^{-1} during the wet season and 2444–3094 μmol kg^{-1} during the dry season at the freshwater end-member.

DIC and TAlk were approximately conservative at salinity >5 in all seasons (Fig. 4). Although DIC and TAlk values and their distribution patterns differed significantly at the upper estuary during dry and wet seasons, they varied much less in the mid and outer estuary with near-shore seawater end-member values around 1850–1940 μmol kg^{-1} for DIC and 2255–2274 μmol kg^{-1} for TAlk (Fig. 4).

The TAlk distribution in the Pearl River estuary is consistent with previous measurements though earlier data have much less spatial and temporal resolution. Peng et al. (1992) surveyed pH and TAlk in the Lingdingyang. Their data also showed higher TAlk in the dry season than in the wet season. Another observation made during the wet season by Li et al. (1999) in September 1994, is similar to our results with low TAlk at the freshwater end-member which increased dramatically within salinity 0–1, but was conservative at salinity >8.

3.3. DIC flux to the South China Sea

The flux or load of riverine constituents can be estimated by measuring the concentrations and discharge rates with time and

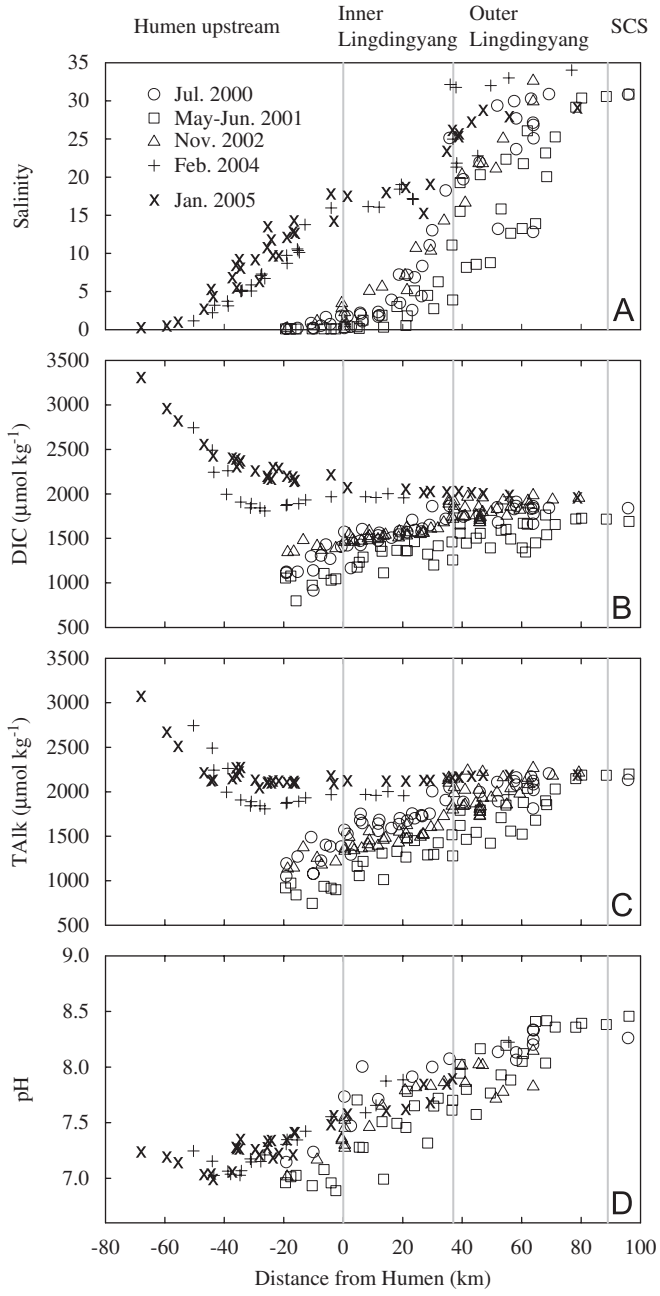

Fig. 3. Spatial distributions of salinity (A), DIC (B), TAlk (C) and pH (D) in the Pearl River estuary. The distance is positive for downstream and negative for upstream of the Humen Outlet. The data for the July 2000 cruise were published in Cai et al. (2004); a few DIC data for May–June 2001 (the 1 June survey) were published in Zhai et al. (2005) and the data in the region of $S<17$ for February 2004 in Dai et al. (2006).

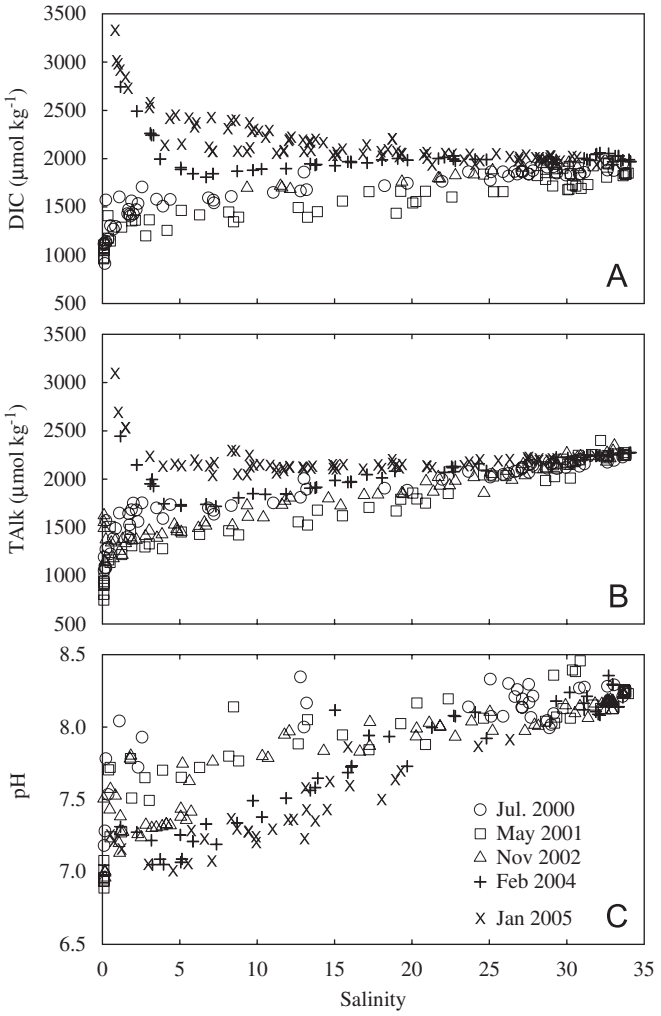

Fig. 4. Salinity distributions of DIC (A), TAlk (B) and pH (C) in the Pearl River estuary.

using statistical models of the concentration/load with river discharge to calculate an annual flux (Cohn et al., 1992; Probst et al., 1992; Gordeev and Sidorov, 1993). The Pearl River is composed of three main tributaries with complex net-like local waterways in the estuarine zone, so that it is difficult to obtain the DIC values of all the end-members over all seasons in order to apply a statistically sound average. We adopted an alternative approach that is often used in estuarine research (Boyle et al., 1974; Kaul and Froelich, 1984; Cai and Wang, 1998; Cai et al., 2004). Thus, we used the effective DIC (C^*_m) extrapolated from the high salinity portion of the estuarine zone to the zero salinity and the total river discharge rate (Q) to estimate the river DIC flux to the SCS (i.e., Flux $= C^*_m \times Q$). This effective concentration represents a composite river end-member of this multiple tributary system as illustrated in Fig. 5, and the 1-m mixing line is described by Eq. (2). The 2-m, m-s, 1-s, 2-s mixing equations are similar, and the effective concentration is calculated from Eq. (3):

$$C_{1\text{-m}} = C^*_1 + (C_m - C^*_1) \times \frac{S}{S_m}, \quad (2)$$

$$C^*_m = \frac{C^*_1 \times Q_1 + C^*_2 \times Q_2}{Q_1 + Q_2}. \quad (3)$$

In the above equations, subscripts 1, 2 and s denote end-members of River 1, River 2 and seawater, respectively. The asterisk (*) represents the effective river concentration (which is the same as the river end-member concentration as no internal source or sink is introduced yet), and C^*_m is a linear combination of C^*_1 and C^*_2.

The validity of this method and a three end-member mixing model in the Pearl River estuary have been previously introduced in Cai et al. (2004) and we will only briefly explain the flux calculation method here. The three end-members are the high carbonate West and North Rivers (1), the low carbonate East River (2) and the SCS (s). Their concentrations are C^*_1, C^*_2 and C_s, respectively. The fluxes of tributaries 1 and 2 are $F_1 = C^*_1 \times Q_1$ and $F_2 = C^*_2 \times Q_2$, where Q_1 and Q_2 are the discharge rates of rivers 1 and 2. Thus, the total flux $F^T = F_1 + F_2$. However, as C^*_1 and C^*_2 (plus other tributaries) were not all measured during our cruises, we

relied on the observed mixing line to derive a composite river end-member (C^*_m). It can be proved that C^*_m is a linear combination of C^*_1 and C^*_2 and the observed data in the high salinity zone are a result of the linear combination of two separate mixing lines of River 1 with seawater and River 2 with seawater, respectively (Cai et al., 2004). Then the total river flux can be estimated by

$$F^T = C^*_m \times Q^T. \quad (4)$$

As the observed DIC is linearly correlated with salinity at $S>10$ in the Pearl River estuary (i.e., in the Lingdingyang), a linear regression of DIC with salinity is used to extrapolate DIC to zero salinity and calculate the effective DIC (C^*_m) in each of the five surveyed months (Table 1).

Using the effective DIC ($C^*_{m\,i}$) and river discharge rate (Q_i) listed in Table 1, we can derive the discharge-weighted DIC* in the wet season (April–October) from the values of July 2000 and May–June 2001; in the dry season (November–March) from the values of February 2004 and January 2005; and the annual average DIC from all the five surveyed months with Eq. (5). We used the annual average DIC calculated above and the annual average discharge in Table 2 to estimate the annual DIC flux with Eq. (4):

$$\overline{C^*_m} = \frac{\sum_{i=1}^{n} C^*_{m\,i} \times Q_i}{\sum_{i=1}^{n} Q_i}. \quad (5)$$

The results are presented in Table 2. The annually discharge-weighted DIC is 1533 μmol kg^{-1} and the annual DIC flux to the SCS is 478×10^9 mol C yr^{-1} (5.7×10^{12} g C yr^{-1}). Most of the DIC flux is carried to the SCS in the wet season. For example, the DIC flux is 2.5 times higher in the wet season than the dry season. The same procedure was applied to TAlk data and the results are consistent with and similar to those for DIC (Table 2).

However, if the annual mean river water discharge rate and the DIC concentration in only one season (either the wet or dry season) are used without factoring in the seasonal variation, a flux of 442×10^9 mol C yr^{-1} (5.3×10^{12} g C yr^{-1}) or 642×10^9 mol C yr^{-1} (7.7×10^{12} g C yr^{-1}) is obtained. These results are either ~9% less than or ~33% higher than those obtained in the above estimation.

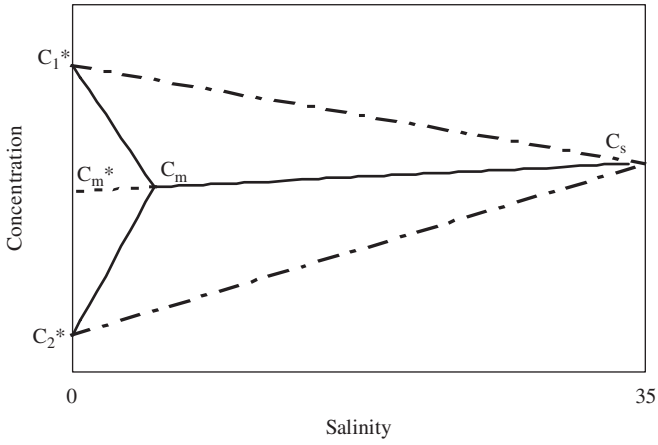

Fig. 5. Three end-member mixing model diagram of the Pearl River estuary. In addition to Eqs. (2) and (3) in the text, the other linear equations are: $C_{2\text{-m}} = C^*_2 + (C_m - C^*_2) \times S/S_m$, $C_{m\text{-s}} = C^*_m + (C_s - C^*_m) \times S/S_s$, $C_{1\text{-s}} = C^*_1 + (C_s - C^*_1) \times S/S_s$, and $C_{2\text{-s}} = C^*_2 + (C_s - C^*_2) \times S/S_s$ (see text for explanation).

4. Discussion

Factors that may contribute to the variations of DIC and TAlk in an estuarine system include mineralogy of the drainage basin, freshwater discharge and weathering intensity, as well as estuarine mixing and biogeochemical processes therein. We will first discuss the drainage basin processes that determine the seasonal variation of the freshwater end-member (i.e., Sections 4.1–4.3). Then, we will explain how mixing of various end-member waters in different seasons can produce a distinctly different pattern in DIC and TAlk distributions in the Pearl River estuary (i.e., Section 4.4). Finally, we will explore possible biogeochemical processes and air–water exchange in the upper estuary that may drive pH and pCO_2 distributions away from their respective mixing lines (i.e., Section 4.5).

4.1. Influence of drainage basin mineralogy

The three main branches of the Pearl River have distinctly different TAlk and DIC concentrations, which is primarily determined by the drainage basin mineralogy. In general, carbonate minerals are less resistant to weathering and thus have a higher weathering rate than silicate minerals (Meybeck, 1987; Amiotte Suchet and Probst, 1995; Amiotte Suchet et al., 2003). The West and North Rivers have much higher TAlk and DIC values than the East River because carbonate weathering dominates in the West and North River drainage basins and silicate weathering is more important in the East River drainage basin (Chen and He, 1999; Li, 2003). Note that the West River basin has the highest $CaCO_3$ mineral content (80%) among all known large river basins (Amiotte Suchet et al., 2003; Cai et al., 2008).

4.2. Influence of river discharge

The balance of precipitation and evaporation plays a central role in modulating the seasonal variation of bicarbonate concentration in the river (Cai et al., 2008). Cai (2003) examined the

Table 2
Effective DIC and TAlk values and their fluxes in the Pearl River in wet and dry seasons

Season	Months	Effective DIC and TAlk (μmol kg^{-1})		Discharge[a] (m^3 s^{-1})	DIC and TAlk flux (10^9 mol C yr^{-1})		Specific DIC and TAlk fluxes[b] (10^5 mol km^{-2} yr^{-1})	
Wet season	7 (April–October)	1450	1456	13,363	611	614	13.6	13.6
Dry season	5 (November–March)	2096	1927	3586	237	218	5.3	4.8
Annual average[c]	12	1533	1480	9894	478	462	10.6	10.3

Note that we used the values of July 2000 and May–June 2001 to derive the wet season DIC (and TAlk) and February 2004 and January 2005 to derive the dry season DIC (and TAlk). November is a transitional season, so it was not included in our calculation of dry season DIC and TAlk concentrations although we classify it as dry season. But for the annual average, we used the data of all the five surveyed months.

[a] Cai et al. (2004).

[b] The area of the Pearl River basin is 4.5×10^5 km^2 (Zhao, 1990).

[c] The annual DIC and TAlk fluxes are calculated from the annual discharge, which is 5% higher than the average of the wet season and dry season.

relationship between the concentration of HCO_3^- and freshwater discharge of the Mississippi River and observed a negative correlation between HCO_3^- concentration and river discharge, suggesting a dilution effect of the relatively stable weathering signal by precipitation in the drainage basin. A similar effect has also been observed for the Congo (Probst et al., 1992), the Changjiang (Li and Zhang, 2003), and the Indus (Karim and Veizer, 2000). Prior investigation has suggested that the HCO_3^- concentration of the East River is negatively correlated with river discharge (Chen and He, 1999). At the same time, the long-term averaged flow rate in January or February accounts for only ~2% of the total annual discharge. In addition, the sampling period of February 2004 and January 2005 (the two black columns in Fig. 2) were ~20% and 11% lower than the long-term monthly average (http://sqqx.hydroinfo.gov.cn/websq/). It is thus clear that the high DIC and TAlk values in the dry season are mainly a result of the much lower freshwater discharge in the sampling periods.

4.3. Change of weathering intensity

Weathering intensity is another important factor affecting the variation of DIC and TAlk. For most river basins, the intensity of chemical weathering increases in the wet season (Gaillardet et al., 1999). High CO_2 consumption by weathering is achieved during the maximum discharge period in the Niger River (Tardy et al., 2004). This is also true in the case of DIC flux into the Mississippi and Changjiang estuaries. Although the DIC values in the Mississippi and Changjiang display a reverse pattern with the discharge rate, the DIC export flux is positively correlated to the discharge rate (Cai, 2003; Li and Zhang, 2003; Cai et al., 2008). In the case of the Pearl River estuary, the area-specific DIC flux is calculated as 13.6 and 5.3×10^5 mol km^{-2} yr^{-1}, respectively, for the wet and dry season (Table 2). Thus, the relative weathering rate in the wet season is 2.5 times that in the dry season.

Extremely high- and low-specific fluxes occur in the peak flow season (summer) and lowest flow season (winter), respectively. The effective DIC concentration in July and February was 1523 and 1840 μmol kg^{-1}, respectively, (Table 1), and the average discharge rate in our July and February sampling periods was 15540 and 1480 m^3 s^{-1}, respectively, at the Wuzhou hydrological station on the West River. If we assume that the West River accounts for ~70% of the freshwater discharge of the Pearl River and use it as a scaling factor, the specific DIC flux of the Pearl River basin is 23.7×10^5 mol km^{-2} yr^{-1} and 2.7×10^5 mol km^{-2} yr^{-1}, respectively, for July and February. Thus, the specific DIC flux, which we take as a measure of drainage basin weathering rate, in July is 8.7 times that in February even though the DIC concentration is lower in the wet season. On the other hand, river discharge rate in July was more than 10 times that in February during our sampling period (Fig. 2 and also http://sqqx.hydroinfo.gov.cn/websq/). Therefore, lower DIC and TAlk values in the wet season at the upper Pearl River estuary is the result of dilution of the intensified weathering rate by high precipitation.

Another probable reason for the higher DIC and TAlk in dry seasons is the relatively larger contribution of groundwater input. Groundwater usually has a much higher DIC signal than surface waters (Dowling et al., 2003; Sarine et al., 1989; Cai et al., 2003; Tardy et al., 2004). Increased discharge from runoff has a dilution effect on the DIC and TAlk values (Atekwana and Krishnamurthy, 1998; Howland et al., 2000). Although we did not collect groundwater samples in this area, nor is there information in the literature concerning groundwater input to the Pearl River estuary, an increased relative contribution from groundwater input could be a viable alternative for higher DIC and TAlk contents in the Pearl River in the dry season. In a broad sense, carbonate dissolution in subsurface aquifers is part of the weathering process in the drainage basin.

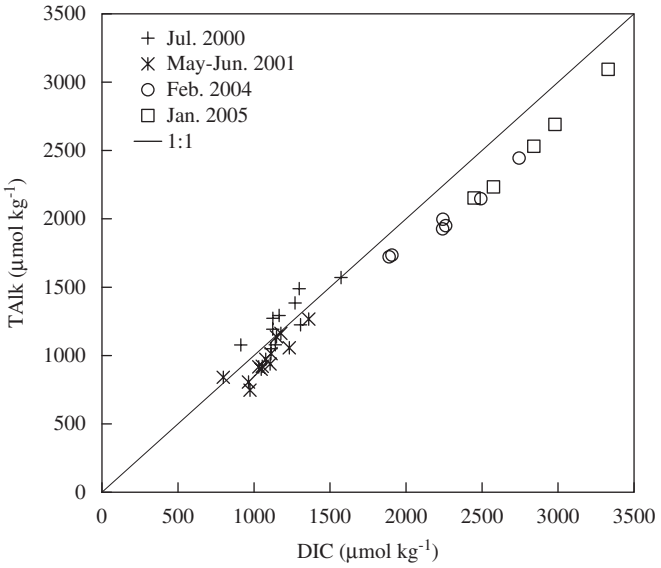

Fig. 6. The relationship of TAlk to DIC in the freshwater end-member ($S<1$ in wet season and $S<3$ in dry season) of the Pearl River estuary.

An interesting feature of the freshwater end-member seasonal variation is the TAlk to DIC ratio. This ratio is generally higher in the wet season (0.9–1.2) than in the dry season (about 0.8) (Fig. 6). This feature is consistent with the postulation of a relatively larger contribution of groundwater to the river carbonate system. Very high pCO_2, relatively low pH and a low TAlk to DIC ratio have been reported for a carbonate groundwater aquifer (Cai et al., 2003). This characteristic of groundwater has been used to interpret the high pCO_2 in rivers (Kempe et al., 1991). When groundwater seeps out to the surface, CO_2 degassing can cause a lower DIC but has no effect on TAlk, and thus the TAlk/DIC ratio increases. During the dry season, as the fraction of rainwater decreases and the fraction of groundwater in stream waters increases, river water may have a higher pCO_2 (which was observed during our dry season) and a lower TAlk to DIC ratio.

4.4. Estuarine mixing

In conjunction with seasonal changes of the end-member characterizations, DIC and TAlk behavior in the estuarine mixing zone can largely be explained with a multiple end-member mixing model which will be instructive for the interpretation of CO_2 parameters in other estuaries. Focusing on the mixing process is often necessary because a complicated mixing schedule tends to mask the biogeochemical processes, which may emerge after unmasking the mixing effect. With three large and several small branches having different drainage basin mineralogy and discharge rates in the upper stream, and many interconnected branches in the estuarine deltaic area, the Pearl River estuarine system is one of the most complex estuaries in the world. To help to delineate the control mechanism behind the observed distribution patterns, the geographic and geological information of branches discharging into the Lingdingyang is simplified in Fig. 7.

For our wet season surveys, the freshwater end-member and the upper stream boundary ended at point B where the East River merges into the main channel (Fig. 7). In contrast, during our dry season surveys, the freshwater end-member and the upper stream end extended to point A which is ~50 km upstream of point B

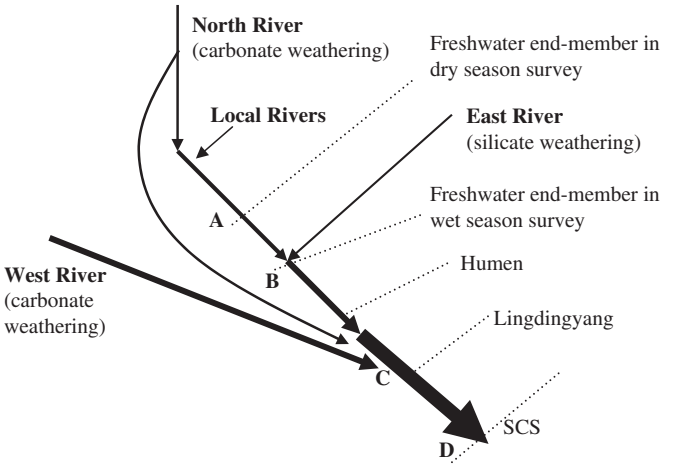

Fig. 7. A simplified illustration of the estuarine mixing scheme in the Pearl River estuary. Point A represents the upper stream freshwater end-member in the dry season, and point B represents the upper stream freshwater end-member in the wet season. The West River is only the part that discharges into the Lingdingyang.

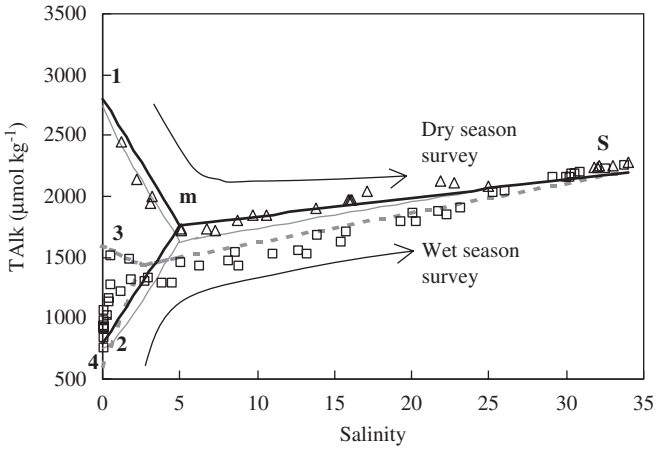

Fig. 8. Model representation of the TAlk distribution pattern vs. salinity based on a three end-member mixing. The arrows give the direction of the surveys from the upstream to the downstream direction. The numbers denote the freshwater end-members. 1 and 3 represent the high carbonate freshwater end-member of the North and/or West Rivers during the dry and wet season, respectively. 2 and 4 represent the low carbonate freshwater end-member of the East River at dry and wet seasons, respectively. Mixing lines are generated from the TAlk values of the three end-members (River 1, River 2 and seawater) as well as the discharge rates of the two rivers based on the mixing model given in Fig. 5. For the wet season, the gray dashed lines denote the conservative mixing lines, and the open squares denote the observed values in May–June 2001; for the dry season, the solid black lines denote the conservative mixing lines; the thin gray solid lines denote the mixing under the influence of nitrification; the "Δ" symbols denote the observed values in February 2004 (the data in the region of $S<17$ are cited from Dai et al., 2006).

(Figs. 1 and 7). The complicated DIC and TAlk relationship with salinity observed in the upper and mid estuarine zone reflects the fact that the freshwater end-member shifted from the low carbonate East River in the wet season to a high carbonate source water further upstream in the dry season. In other words, the different DIC or TAlk to salinity patterns reflect two different mixing schemes. During wet seasons, DIC and TAlk were low, starting from the East River value (point B) and increased downstream with salinity to a higher value at point C where the North River and a branch of the West River discharge into the inner Lingdingyang. During dry season surveys, DIC and TAlk values were high at point A, above which a branch of the North River mixed with several local rivers, and decreased rapidly towards low values at point B where the East River merges into the main channel. Further downstream in the inner Lingdingyang, because of the very limited flow of the West and North Rivers in the dry season, the high DIC and TAlk delivered by these rivers could not be detected in the main channel of the Lingdingyang where samples were collected.

This mixing scheme is illustrated in a TAlk-to-salinity plot using the five parameters of the three end-members (i.e., three TAlk values and two discharge rates of rivers 1 and 2) in Fig. 8. The DIC–salinity distribution is similar (not presented) using the same five parameters and an appropriate DIC to TAlk ratio for each river (Fig. 6). The mixing model equations are presented in Section 3.3, and the end-member values are in Table 3. The above mixing mechanism satisfactorily explains why we observed a low DIC and TAlk freshwater end-member that increased rapidly with salinity in the wet season surveys and a high freshwater end-member that decreased rapidly with salinity in the dry season surveys (i.e., following their respective survey routes indicated in Fig. 8). The observed values in May–June 2001 and February 2004 are also shown in Fig. 8. The simulated values and the observations are reasonably consistent.

In addition to the consistent geochemical signals of the carbonate system presented and discussed in the above sections, additional supporting information comes from the November 2002 survey which was in the beginning of the dry season when river discharge was still relatively high (Fig. 2). While we did not sample beyond the 0 salinity end-member (i.e., beyond the East River mouth), we sampled end-member values in three waterways in the inner Lingdingyang through which branches of the West and North Rivers discharge into the estuary. High TAlk was measured in these water outlets ($S = 0.1$) (Fig. 9A). These results support the assumption of high TAlk and DIC values in the West and North Rivers in addition to upper stream data (Figs. 3 and 4). The TAlk vs. salinity plot from November 2002 (Fig. 9B) clearly illustrates that the proposed three end-member mixing scheme is correct.

Table 3
End-member parameters of the three end-member mixing model

	Q_1 ($m^3 s^{-1}$)	Q_2 ($m^3 s^{-1}$)	C_1 ($\mu mol\ kg^{-1}$)	C_2 ($\mu mol\ kg^{-1}$)	C_s ($\mu mol\ kg^{-1}$)
Wet season	3650	1070	1600	600	2200
Dry season	350	440	2800	800	2200

The river discharge data are cited from Cai et al. (2004). In the wet season, the mixing mainly occurs at the Inner Lingdingyang near Humen, so we use the discharge of (Humen+Jiaomen-East River) as the discharge of River 1 and the discharge from East River as the discharge of River 2; in the dry season, the mixing mainly occurs at the upper Humen area, so the difference of discharges from Humen and East River is used as the discharge of River 1 and East River as River 2. Chen and He (1999) reported the long-term average HCO_3^- of North River and East River as 1560 and 624 $\mu mol\ L^{-1}$. We use 1600 and 600 $\mu mol\ L^{-1}$ as the wet season and 2800 and 800 $\mu mol\ L^{-1}$ as the dry season end-members according to Chen and He (1999) and our observations.

However, the above mixing mechanism alone is not sufficient to explain the pH minimum (Fig. 4C) and pCO_2 maximum observed near the metropolitan areas during our dry season surveys. Additional processes that changed the acid-base property of the water must have occurred and altered the pH and pCO_2 signals, although the less sensitive total concentration properties such as DIC and TAlk are largely explained by the mixing processes of the drastically different end-members.

4.5. Biogeochemical processes

Processes that may drawdown DIC include biological uptake (or photosynthesis) and CO_2 evasion to the atmosphere. Sources of

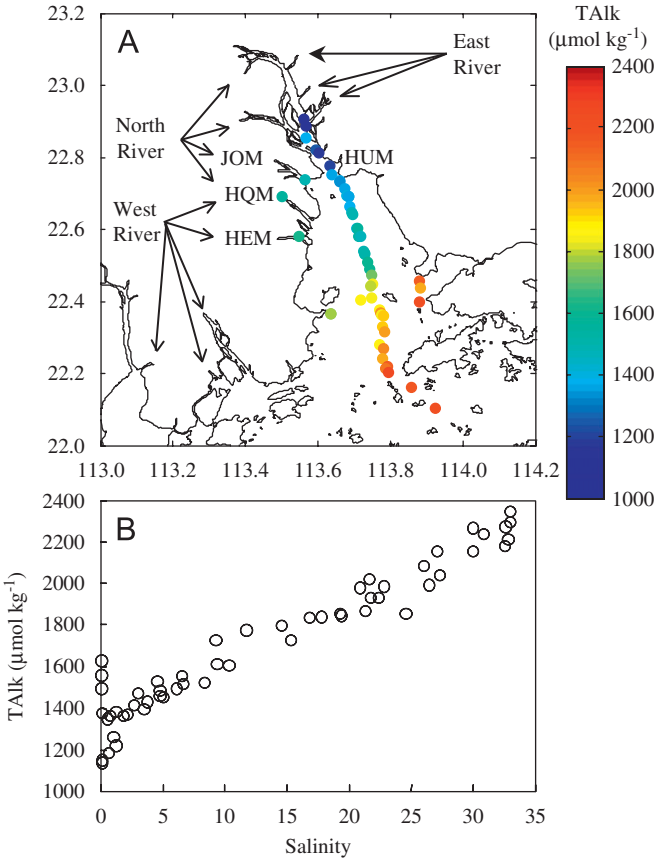

Fig. 9. Spatial distribution of TAlk (A) and salinity distribution of TAlk (B) in the Pearl River estuary in November 2002. Jiaomen (JOM) and Hongqimen (HQM) are outlets of the North River, and Hengmen (HEM) is an outlet of the West River. A branch of the West River also discharges through Hongqimen. As these outlets are interconnected and have similar carbonate properties, they are represented as one end-member in Figs. 7 and 8.

DIC include aerobic respiration and denitrification. Another important process is nitrification which lowers TAlk and pH, but has no effect on DIC.

4.5.1. Aerobic respiration

Aerobic respiration is an important mechanism to maintain high pCO_2, low pH and low O_2 levels in the upper estuary (Zhai et al., 2005; Dai et al., 2006; Cai et al., 1999). However, while aerobic respiration may be an important process contributing to DIC, it has little effect on alkalinity (i.e., $(CH_2O)_{106}(NH_3)_{16}(H_3PO_4)+138O_2 \rightarrow 106CO_2+16HNO_3+H_3PO_4+122H_2O$). Thus, it cannot be used to explain the sharp and simultaneous decrease in DIC and TAlk in the upper estuarine mixing zone observed in this study. This argument is not in conflict with our earlier results that high pCO_2 is maintained by aerobic respiration (Zhai et al., 2005; Dai et al., 2006), as molecular CO_2 is an important but small fraction of DIC. For example, at a pCO_2 level of 6000 μatm in the upper stream (Dai et al., 2006), $[CO_2]$ is about 200 μmol kg^{-1}, which is less than 10% of the DIC in dry seasons. A change of 100 μmol kg^{-1} in $[CO_2]$ would alter greatly the pCO_2 and pH signals (and $[O_2]$ if the cause is aerobic respiration), but is hardly discernable in the DIC–salinity mixing diagram since the total decrease in DIC due to mixing is about 1000 μmol kg^{-1} in the dry season (see further discussion in the pH section). The total oxygen consumption rate determined in shipboard incubations was 22.5 mmol O_2 m^{-3} d^{-1} in February 2004 in the upper Pearl River estuary (Dai et al., 2006). As the water depth is about 5 m (Guangzhou Chorography Compilation Committee, 1998) and the $\Delta DIC/-\Delta[O_2]$ ratio is 0.62–0.79 (Zhai et al., 2005), the CO_2 production rate would be 14–18 mmol m^{-3} d^{-1}. With a water travel time of 5–10 days in the upper estuary in the dry season (see Section 3.1), the DIC addition would be small (i.e., 70–180 μmol kg^{-1} or 70–90 mmol m^{-2} d^{-1}).

4.5.2. CO_2 evasion

pCO_2 was very high, particularly during the dry season, in the upper estuarine zone. Thus, degassing is expected to be significant. CO_2 evasion to the atmosphere, however, cannot explain the rapid and simultaneous decrease of DIC and TAlk with salinity as it does not affect TAlk. In addition, CO_2 evasion is an unlikely candidate for fully explaining the DIC decrease. CO_2 efflux in the upper Pearl River estuary ($S<3$) calculated using the field wind speed and the formula of Wanninkhof (1992) is only 61 mmol m^{-2} d^{-1} (or 12 mmol m^{-3} d^{-1} in a 5-m water column). Thus, the CO_2 production process due to aerobic respiration (70–90 mmol m^{-2} d^{-1}) will completely compensate for the DIC loss due to CO_2 outgassing.

Higher CO_2 evasion rates can be estimated using other gas transfer formula (see discussion in Raymond and Cole, 2001). CO_2 losses of 208 and 476 mmol m^{-2} d^{-1} (or 42 and 95 mmol m^{-3} d^{-1}) were estimated with the formulae of Raymond and Cole (2001) and Borges et al. (2004). However, a decrease in DIC of 100 μmol kg^{-1} while holding TAlk constant, would result in a pH increase of 0.35 units which is opposite to what was observed in the field (i.e., a pH decrease). Thus, the true field CO_2 degassing rate is perhaps not much greater than that predicted by the Wanninkhof (1992) formula and causes no significant pH increase. Thus, we will assume that the gas evasion should be within three times that predicted by the Wanninkhof (1992) equation.

4.5.3. Nitrification and denitrification

Nitrification and denitrification are important biogeochemical processes in the upper Pearl River estuary (Dai et al., 2006). The ammonium (NH_4^+) concentration reached >600 μmol kg^{-1} in the upper Pearl River estuary near Guangzhou during the dry season, likely associated with industrial and municipal wastewater discharge (Dai et al., 2006). Its concave downward shape in the plot of NH_4^+ against salinity suggests the possibility of strong removal via nitrification in the dry season. A significant nitrification rate in surface water was also measured during the January 2005 cruise (~5 mmol m^{-3} d^{-1}, Dai et al., unpublished data) and in sediment (58.3 mmol m^{-2} d^{-1}) in March 2004 in the same area near Guangzhou (Xu et al., 2005). Taking an average water depth of 5 m, the sediment nitrification rate can be converted to a water column rate of 11.7 mmol m^{-3} d^{-1} assuming there is a strong benthic-pelagic coupling in such a shallow and dynamic system. Thus, the overall pelagic and benthic nitrification rate may be as high as 17 mmol m^{-3} d^{-1}. The ratio of $\Delta TAlk/\Delta[NH_4^+]$ during nitrification is 2 (i.e., $NH_4^+ + 2O_2 \rightarrow NO_3^- + 2H^+ + H_2O$), and thus its influence on alkalinity change would be $\Delta TAlk = -34$ mmol m^{-3} d^{-1}. However, nitrification has no effect on DIC.

Xu et al. (2005) determined a denitrification rate of 20.2 mmol m^{-2} d^{-1} in the sediment (which can be converted to a water column-based value of 4.0 mmol m^{-3} d^{-1}). Assuming there is no denitrification in the water column since the water column is generally oxygenated, we used 4.0 mmol m^{-3} d^{-1} as the overall denitrification rate. As denitrification increases TAlk and DIC in roughly a 1:1 ratio to NO_3^- reduction ($\Delta TAlk/\Delta[NO_3^-] = -1.17$ and $\Delta DIC/\Delta[NO_3^-] = -1.25$, following the formula $(CH_2O)_{106}(NH_3)_{16}(H_3PO_4)+0.8 \times 106NO_3^- + 0.8 \times 106H^+ \rightarrow 106CO_2+0.4 \times 106N_2+16NH_3+H_3PO_4+1.4 \times 106H_2O$; Van Cappellen and Wang, 1996), then $\Delta TAlk = 4.0$ mmol m^{-3} d^{-1}. Thus, the net effect of nitrification and

denitrification on TAlk change would be about $-30\,mmol\,m^{-3}\,d^{-1}$ (or $\mu mol\,kg^{-1}\,d^{-1}$). With a water transit time of 5–10 days, the total amount of acid generated, or TAlk reduction, can be up to 150–300 $\mu mol\,kg^{-1}$. Similarly estimated, the net effect of denitrification on DIC would be small (with only an increase of 20–40 $\mu mol\,kg^{-1}$).

Based on the curvilinear regression of $[NH_4^+]$ and its first-order derivative in the upper Pearl River estuary ($S = 1$–5), Dai et al. (2006) calculated that the dilution-corrected $\Delta[NH_4^+]$ (i.e., apparent NH_4^+ removal) is $-153\,\mu mol\,kg^{-1}$ in the upper estuarine zone (salinity 1–5). If a water transit time of 5–10 days is used, this value would be translated into a nitrification rate of ~15–31 $mmol\,m^{-3}\,d^{-1}$, which is not greatly different from the estimate here ($17\,mmol\,m^{-3}\,d^{-1}$) that is based on the incubation measurements of Dai et al. (2006) and Xu et al. (2005).

4.5.4. Carbonate dissolution

$CaCO_3$ was under saturated in the upper Pearl River estuary in February 2004 (Dai et al., 2006). Thus, possible $CaCO_3$ dissolution may affect DIC and TAlk with a mole ratio of 1:2 (i.e., $CaCO_3(s)+CO_2+H_2O \rightarrow Ca^{2+}+2HCO_3^-$). But its effect on DIC and TAlk is difficult to quantify.

4.5.5. Photosynthesis

High turbidity (data not shown) in the upper estuarine water prevented significant biological production. The very low DO ($<20\,\mu mol\,kg^{-1}$; Dai et al., 2006) also suggests no significant primary production in the upper estuary.

To sum up, CO_2 evasion may remove 60–360 $\mu mol\,kg^{-1}$ of DIC from the upper Pearl River estuary (Table 4). On the other hand, since aerobic respiration and denitrification may add 70–180 $\mu mol\,kg^{-1}$ and 20–40 $\mu mol\,kg^{-1}$ of DIC, respectively, to the system, the net effect of the CO_2 evasion and biogeochemical processes is not significant relative to the apparent DIC reduction (~1000 $\mu mol\,kg^{-1}$) in the upper Pearl River estuary. However, since the uncertainties of rates in aerobic respiration and gas evasion are compounded by the uncertainty in the water transit time, the precise estimation of net DIC change is not possible (see Table 4). The possible $CaCO_3$ dissolution also makes it more difficult to precisely quantify the carbonate system. We thus assume that the CO_2 production during both aerobic respiration and denitrification is roughly balanced by the CO_2 loss due to gas evasion. Based on the following two arguments, we believe this assumption is reasonable. First, in a simplistic view, if CO_2 addition due to respiration exceeds the CO_2 loss due to gas evasion, then water pCO_2 would increase until a new balance is reached. Second, the composite river end-member DIC value extrapolated from the high salinity estuarine zone actually agrees with that calculated from the upper stream information (i.e, DIC and discharge of the tributaries) (Cai et al., 2004). Thus, it appears that no significant net addition or removal of DIC has occurred in the estuarine mixing process.

Table 4
Estimated effects of estuarine processes on TAlk and DIC in the upper and mid sections of the Pearl River estuary

Process	TAlk		DIC	
	$mmol\,m^{-3}\,d^{-1}$	$mmol\,m^{-3}$	$mmol\,m^{-3}\,d^{-1}$	$mmol\,m^{-3}$
Photosynthesis	–	–	–	–
Aerobic respiration	~0	~0	14-18	70–180
CO_2 evasion	0	0	−36[a] to −12	−360 to −60
Nitrification	−34	−340 to −170	0	0
Denitrification	4	20–40	4	20–40
Net result	−30	−300 to −150	−18 to 10	−140 to 30

A positive value indicates gain and negative loss. In the net result, ranges with largest possible error are given. A 5-m water depth is applied and a 5- to 10-day water transit time is assumed. See text for explanations.

[a] Three times the CO_2 evasion calculated from Wanninkhof (1992).

For TAlk, the net effect of nitrification and denitrification is a removal of 150–300 $\mu mol\,kg^{-1}$ (Table 4), which cannot be discerned with confidence in the TAlk vs. salinity plot. Therefore, most of the apparent DIC and TAlk decrease in the dry season is the result of dilution by the low carbonate East River. The model simulated TAlk values are very similar to the observations (Fig. 8), which confirmed that the effects of biogeochemical processes on the distribution of TAlk and DIC are limited relative to the dramatic mixing process.

However, the mixing mechanism alone is not sufficient to explain the pH minimum (Figs. 3D and 4C) and pCO_2 maximum observed during dry season surveys. Although the biogeochemical processes discussed above make only small and variable contributions to DIC and TAlk, they can significantly alter pH and pCO_2. Perhaps the strongest evidence to support an influence of nitrification and denitrification on the carbonate system is the pH minimum and the pCO_2 maximum at the upper estuary in the dry season. While this was recognized in our earlier paper (Dai et al., 2006), it was not quantitatively demonstrated nor proved to be the right mechanism. As discussed above, the net DIC change was not significant under the influence of biological processes, but the net TAlk change is a reduction of 150–300 $\mu mol\,kg^{-1}$ largely due to NH_4^+ oxidation. Thus, we may simulate the distributions of pH and pCO_2 based on the three end-member mixing model with a reasonable TAlk reduction of up to 150 $\mu mol\,kg^{-1}$. The simulations were carried out using the CO2sys program (Lewis and Wallace, 1998) with the following inputs: average field temperature (25 °C for the wet season and 15 °C for the dry season), salinity, silicate (data not shown), TAlk, and DIC values generated by the same five parameters given in Fig. 8 and Table 3. The TAlk reduction from the conservative mixing line is determined from the nitrification rates at low and intermediate salinities measured by Dai et al. (unpublished data). The TAlk reduction is 50, 150, and 0 $\mu mol\,kg^{-1}$, respectively, at salinities of 0, 2, and 25. The values of TAlk reduction at other salinities were derived based on a linear increase at salinity <2 and a linear decrease at salinity >2 (shown as solid light thin lines in Fig. 8). The simulated pH and pCO_2 are shown in Fig. 10. Clearly, one cannot simulate the observed pH minimum and pCO_2 maximum based on the conservative mixing model alone (black solid lines in Fig. 10). A reasonably small additional non-conservative TAlk decrease (up to 150 $\mu mol\,kg^{-1}$) relative to a conservative DIC value generates the patterns of pH and pCO_2 changes we observed in the dry season. Such a small non-conservative extra TAlk decrease cannot be discerned with confidence by a direct examination of measured TAlk and DIC data (i.e., how much the property–salinity plot deviates from the conservative lines in Fig. 8). However, its influence is evident from the above pH simulation. This conclusion is further supported by a TAlk/DIC ratio plot (Fig. 11). This ratio dips from 0.95 near zero salinity to 0.86 at a salinity of 2.5 before increasing towards the outer estuary in the dry season. A change in the TAlk to DIC ratio from 0.95 to 0.86 is equivalent to a decrease of 200 $\mu mol\,kg^{-1}$ in TAlk relative to DIC. The insert in Fig. 11 also illustrates that pH is strongly controlled by the ratio of TAlk to DIC in the specific estuary. Further research is needed to strengthen the link between nitrification rates and the occurrence of the pH minimum and pCO_2 maximum in the Pearl River and other similar systems.

It is not our intention for the modeled values to match completely the observations, since the complex biological processes are hard to accurately quantify and, at the same time, the net-like channels of the Pearl River system also make the

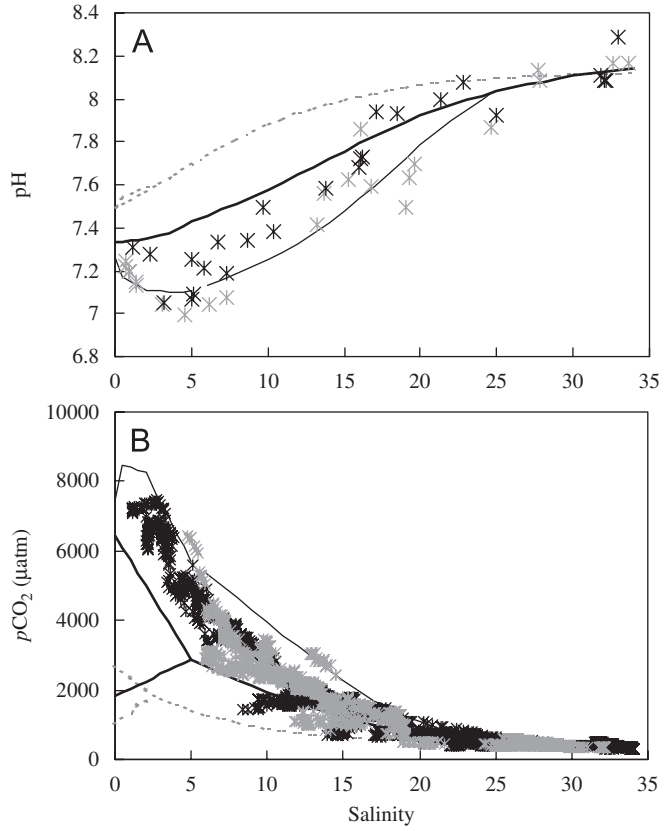

Fig. 10. A mechanistic explanation of the effect of nitrification on the formation of pH minimum (A) and pCO_2 maximum (B) during the dry season. For the dry season simulation, the solid black lines are the result of conservative mixing among the three end-members; the gray solid lines (same symbols as in Fig. 8) represent those with the effect of nitrification in dry season as explained in the text; the black and gray "*" symbols represent February 2004 and January 2005 data, respectively. For the wet season simulation, only conservative mixing (dashed gray lines) is presented since nitrification is not significant in the mixing zone.

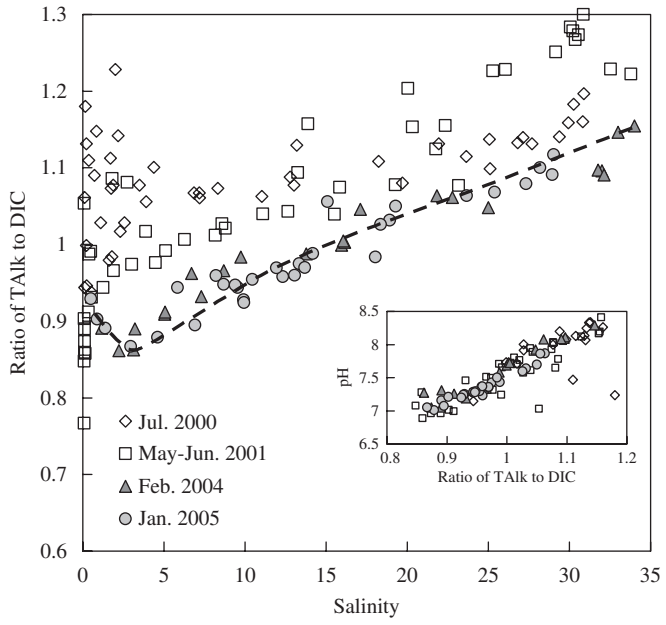

Fig. 11. Variation in the TAlk to DIC ratio with salinity. A strong correlation between pH and the TAlk/DIC ratio is shown in the inserted figure in the low-right corner. For the two dry season surveys (February 2004 and January 2005), R^2 values are 0.92 and 0.94, respectively.

simulation difficult. The above modeling is chosen to illustrate the pH regulation mechanism rather than to strictly simulate the exact pH and pCO_2 changes.

5. Concluding remarks

In the Pearl River estuary, both DIC and TAlk have higher values in the dry season than in the wet season. While maximum chemical weathering rate is 8.7 times higher in July than in February, the dilution effect, due to higher discharge, caused lower DIC and TAlk values in the estuary during the wet season.

A combination of shifting between two mixing regimes and the variation of end-member DIC and TAlk values between the dry and wet seasons are the main causes for the observed complicated mixing diagram of carbonate parameters in the Pearl River estuarine water. In conjunction, biogeochemical processes actively modify carbonate signals (in particular pH and pCO_2) in the upper estuarine zone during the dry season.

The seasonal average of annual DIC flux from the Pearl River to the SCS is 478×10^9 mol C yr^{-1} (5.7×10^{12} g C yr^{-1}). Significant uncertainty (−9% to +33%) can be incurred if this seasonal variability of the inorganic carbon system is not considered.

Acknowledgments

This work was supported by the Natural Science Foundation of China (NSFC) through grants #49825111, #40228007, #40576036, #40521003 and #90211020. Preparation of this paper was supported by US NSF grant OCE-0425153 (awarded to W.-J. Cai) under which X.-H. Guo was a visiting student at the University of Georgia. We thank the crew of R.V. *Yanping II* and W.-Q. Ruan for their assistance during the sampling cruise. Z.-Z. Chen collected CTD data; P.-H. Cai collected end-member samples in three waterways to the inner Lingdingyang; Z.-M. Lu collected the TAlk and pH data in the May–June 2001 and November 2002 cruises. Comments made by three anonymous reviewers improved the quality of this paper greatly. Finally, we thank Professors P. Harrison for editing and J. Hodgkiss for English assistance.

References

Abril, G., Borges, A.V., 2004. Carbon dioxide and methane emissions from estuaries. In: Tremblay, A., Varfalvy, L., Roehm, C., Garneau, M. (Eds.), Greenhouse Gases Emissions from Natural Environments and Hydroelectric Reservoirs: Fluxes and Processes, Chapter 7, pp. 187–207.

Amiotte Suchet, P., Probst, J.-L., 1995. A global model for present-day atmospheric/soil CO_2 consumption by chemical erosion of continental rocks (Gem-CO_2). Tellus Series B 47, 273–280.

Amiotte Suchet, P., Probst, J.-L., Ludwig, W., 2003. World distribution of continental rock lithology: implications for the atmospheric/soil CO_2 uptake by continental weathering and alkalinity river transport to the oceans. Global Biogeochemical Cycles 17 (2), 1038.

Atekwana, E.A., Krishnamurthy, R.V., 1998. Seasonal variations of dissolved inorganic carbon and $\delta^{13}C$ of surface waters: application of modified gas evolution technique. Journal of Hydrology 205, 265–278.

Borges, A.V., Vanderborght, J.P., Schiettecatte, L.S., Gazeau, F., Ferron-Smith, S., Delille, B., Frankignoulle, M., 2004. Variability of the gas transfer velocity of CO_2 in a macrotidal estuary (the Scheldt). Estuaries 27, 593–603.

Boyle, E., Collier, R., Dengler, A.T., Edmond, J.M., Ng, A.C., Stallard, R.F., 1974. On the chemical mass-balance in estuaries. Geochimica et Cosmochimica Acta 38, 1719–1728.

Cai, W.-J., 2003. Riverine inorganic carbon flux and rate of biological uptake in the Mississippi River plume. Geophysical Research Letters 30(2), 1032, doi:10.1029/2002GL016312.

Cai, W.J., Wang, Y., 1998. The chemistry, fluxes, and sources of carbon dioxide in the estuarine waters of the Satilla and Altamaha rivers, Georgia. Limnology and Oceanography 43, 657–668.

Cai, W.J., Pomeroy, L.R., Moran, M.A., Wang, Y.C., 1999. Oxygen and carbon dioxide mass balance for the estuarine-intertidal marsh complex of five rivers in the southeastern US. Limnology and Oceanography 44, 639–649.

Cai, W.-J., Wang, Y., Krest, J., Moore, W.S., 2003. The geochemistry of dissolved inorganic carbon in a surficial groundwater aquifer in North Inlet, South Carolina and the carbon fluxes to the coastal ocean. Geochimica et Cosmochimica Acta 67, 631–637.

Cai, W.-J., Dai, M.H., Wang, Y.C., Zhai, W.D., Huang, T., Chen, S.T., Zhang, F., Chen, Z.Z., Wang, Z.H., 2004. The biogeochemistry of inorganic carbon and nutrients in the Pearl River estuary and the adjacent Northern South China Sea. Continental Shelf Research 24, 1301–1319.

Cai, W.-J., Guo, X., Chen, C.-T.A., Dai, M., Zhang, L., Zhai, W., Lohrenz, S.E., Wang, Y., 2008. A comparative overview of weathering intensity and HCO_3^- flux in the world's major rivers with emphasis on the Changjiang, Huanghe, Pearl and Mississippi Rivers. Continental Shelf Research, in press, doi:10.1016/j.csr.2007.10.014.

Chen, J., He, D., 1999. Chemical characteristics and genesis of major ions in the Pearl River basin. Acta Scientiarum Naturalium Universitatis Pekinesis 35, 786–793 (in Chinese).

Cohn, T.A., Caulder, D.L., Gilroy, E.J., Zynjuk, L.D., Summers, R.M., 1992. The validity of a simple statistical-model for estimating fluvial constituent loads—an empirical-study involving nutrient loads entering Chesapeake Bay. Water Resources Research 28, 2353–2363.

Dai, M.H., Guo, X.H., Zhai, W.D., Yuan, L.Y., Wang, B.W., Wang, L.F., Cai, P.H., Tang, T.T., Cai, W.-J., 2006. Oxygen depletion in the upper reach of the Pearl River estuary during a winter drought. Marine Chemistry 102, 159–169.

Degens, E.T., Kempe, S., Richey, J.E., 1991. Summary: biogeochemistry of major world rivers. In: Degens, E.T., Kempe, S., Richey, J.E. (Eds.), Biogeochemistry of Major World Rivers. SCOPE Report 42. Wiley, Chichester, New York, pp. 323–347.

Dowling, C.B., Poreda, R.J., Basu, A.R., 2003. The groundwater geochemistry of the Bengal Basin: weathering, chemsorption, and trace metal flux to the oceans. Geochimica et Cosmochimica Acta 67, 2117–2136.

Frankignoulle, M., Abril, G., Borges, A., Bourge, I., Canon, C., DeLille, B., Libert, E., Theate, J.M., 1998. Carbon dioxide emission from European estuaries. Science 282, 434–436.

Gaillardet, J., Dupre, B., Laouvat, P., Allegre, C.J., 1999. Global silicate weathering and CO_2 consumption rates deduced from the chemistry of large rivers. Chemical Geology 159, 3–30.

Gieskes, J.M., 1969. Effect of temperature on the pH of seawater. Limnology and Oceanography 14, 679–685.

Gordeev, V.V., Sidorov, I.S., 1993. Concentrations of major elements and their outflow into the Laptev Sea by the Lena River. Marine Chemistry 43, 33–45.

Grasshoff, K., Ehrhardt, M., Kremling, K., Anderson, L.G., 1999. Methods of Seawater Analysis. Wiley-VCH, Weinheim, New York, 632pp.

Guangzhou Chorography Compilation Committee, 1998. Guangzhou Chorography, Natural Geography Record. Guangzhou Publishing House, Guangzhou (in Chinese). 〈http://www.gzsdfz.org.cn〉.

Howland, R.J.M., Tappin, A.D., Uncles, R.J., Plummer, D.H., Bloomer, N.J., 2000. Distributions and seasonal variability of pH and alkalinity in the Tweed estuary, UK. Science of the Total Environment 251, 125–138.

Karim, A., Veizer, J., 2000. Weathering processes in the Indus River Basin: implication from riverine carbon, sulfur, oxygen, and strontium isotopes. Chemical Geology 170, 153–177.

Kaul, L.W., Froelich, P.N., 1984. Modeling estuarine nutrient geochemistry in a simple system. Geochimica et Cosmochimica Acta 48, 1417–1433.

Kempe, S., Pettine, M., Cauwet, G., 1991. Biogeochemistry of European rivers. In: Degens, E.T., Kempe, S., Richey, J.E. (Eds.), Biogeochemistry of Major World Rivers. SCOPE Report 42. Wiley, Chichester, New York, pp. 169–211.

Lewis, E., Wallace, D.W.R., 1998. Program Developed for CO_2 System Calculations. ORNL/CDIAC-105. Carbon Dioxide Information Analysis Center, Oak Ridge National Laboratory, US Department of Energy, Oak Ridge, TN.

Li, J.-Y., 2003. A study on the chemical weathering, mechanical denudation correlative with river water and sediment geochemistry and CO_2 consumption budget and controlling factors in the major drainage basins of China. Doctoral Dissertation, Ocean University of China, Qingdao, China, 195pp. (in Chinese).

Li, J.-Y., Zhang, J., 2003. Variations of solid content and water chemistry at Nantong station and weathering processes of the Changjiang watershed. Resources and Environment in the Yangtze Basin 12, 363–369 (in Chinese).

Li, F., Chen, G., Ji, H., 1999. The alkalinity of seawater in Zhujiang River estuary. Journal of Ocean University of Qingdao (Suppl.), 49–54 (in Chinese).

Meybeck, M., 1987. Global chemical-weathering of surficial rocks estimated from river dissolved loads. American Journal of Science 287, 401–428.

Millero, F.J., 1984. The conductivity–density–salinity–chlorinity relationships for estuarine waters. Limnology and Oceanography 29, 1317–1321.

Peng, Y., Wang, Z., Yi, Z., 1992. The carbon dioxide in the Zhujiang estuarine waters. Environmental Chemistry 11, 56–60 (in Chinese).

Probst, J.L., Nkounkou, R.R., Krempp, G., Bricquet, J.P., Thiebaux, J.P., Olivry, J.C., 1992. Dissolved major elements exported by the Congo and the Ubangi rivers during the period 1987–1989. Journal of Hydrology 135, 237–257.

PRWRC/PRRCC, 1991. The Pearl River Records (Zhujiang Zhi), vol. 1. Guangdong Science & Technology Press, Guangzhou, 150pp. (in Chinese).

Raymond, P.A., Cole, J.J., 2001. Gas exchange in rivers and estuaries: choosing a gas transfer velocity. Estuaries 24, 312–317.

Richey, J.E., Melack, J.M., Aufdenkampe, A.K., Ballester, V.M., Hess, L.L., 2002. Outgassing from Amazonian rivers and wetlands as a large tropical source of atmospheric CO_2. Nature 416, 617–620.

Sarine, M.M., Krishanswami, S., Dilli, K., Somayajulu, B.L.K., Moore, W.S., 1989. Major ion chemistry of the Ganga–Brahmaputra river system: weathering processes and fluxes to the Bay of Bengal. Geochimica et Cosmochimica Acta 53, 997–1009.

Tardy, Y., Bustillo, V., Boeglin, J.L., 2004. Geochemistry applied to the watershed survey: hydrograph separation, erosion and soil dynamics. A case study: the basin of the Niger River, Africa. Applied Geochemistry 19, 469–518.

Van Cappellen, P., Wang, Y.F., 1996. Cycling of iron and manganese in surface sediments: a general theory for the coupled transport and reaction of carbon, oxygen, nitrogen, sulfur, iron, and manganese. American Journal of Science 296, 197–243.

Wanninkhof, R., 1992. Relationship between wind speed and gas exchange over the ocean. Journal of Geophysical Research-Oceans 97 (C5), 7373–7382.

Wong, M.H., Cheung, K.C., 2000. Pearl River estuary and Mirs Bay, south China. In: Dupra, V., Smith, S.V., Marshall Crossland, J.I., Crossland, C.J. (Eds.), Estuarine Systems of the South China Sea Region: Carbon, Nitrogen and Phosphorus Fluxes. LOICZ Reports and Studies 14. LOICZ, Texel, The Netherlands, pp. 7–16.

Xu, J., Wang, Y., Yin, J., Wang, Q., Zhang, F., He, L., Sun, C., 2005. Transformation of dissolved inorganic nitrogen species and nitrification and denitrification processes in the near sea section of Zhujiang River. Acta Scientiae Circumstantiae 25, 686–692 (in Chinese).

Zhai, W., Dai, M., Cai, W.-J., Wang, Y., Wang, Z., 2005. High partial pressure of CO_2 and its maintaining mechanism in a subtropical estuary: the Pearl River estuary, China. Marine Chemistry 93, 21–32.

Zhao, H., 1990. Evolution of the Pearl River Estuary. Ocean Press, Beijing, 357pp. (in Chinese).